Orig Life Evol Biosph (2016) 46:455–471
DOI 10.1007/s11084-016-9498-x

ASTROBIOLOGY

Searching for the Source Crater of Nakhlite Meteorites

A. Kereszturi[1] · **E. Chatzitheodoridis**[2]

Received: 15 August 2015 / Accepted: 16 March 2016 /
Published online: 28 March 2016

Abstract We surveyed the Martian surface in order to identify possible source craters of the nakhlite Martian meteorites. We investigated rayed craters that are assumed to be younger than 11 Ma, on lava surfaces with a solidification age around 1.2 Ga. An area of 17.3 million km^2 Amazonian lava plains was surveyed and 53 rayed craters were identified. Although most of them are smaller than the threshold limit that is estimated as minimum of launching fragments to possible Earth crossing trajectories, their observed size frequency distribution agrees with the expected areal density from cratering models characteristic for craters that are less than few tens of Ma old. We identified 6 craters larger than 3 km diameter constituting the potentially best source craters for nakhlites. These larger candidates are located mostly on a smooth lava surface, and in some cases, on the earlier fluvial-like channels. In three cases they are associated with fluidized ejecta lobes and rays – although the rays are faint in these craters, thus might be older than the other craters with more obvious rays. More work is therefore required to accurately estimate ages based on ray system for this purpose. A more detailed search should further link remote sensing Martian data with the in-situ laboratory analyses of Martian meteorites, especially in case of high altitude, steep terrains, where the crater rays seems to rarely survive several Ma.

Keywords Meteorite · Mars · Nakhlites · Crater · Impact ejection

Introduction

The link of Martian remote sensing data with laboratory analysis of Martian meteorites can provide an effective method to broaden the understanding of the geology of the red planet by improving the quality of interpretation of remote sensing data and also setting constraints in

Paper presented at the conference: Habitability in the Universe: From the Early Earth to Exoplanets, 22–27 March 2015, Porto, Portugal.

✉ A. Kereszturi
kereszturi.akos@csfk.mta.hu

[1] Research Centre for Astronomy and Earth Sciences, Budapest, Hungary

[2] National Technical University of Athens, Athens, Greece

investigating possible past or present life on the planet. Thus the identification and analysis of source areas (i.e., craters) of certain Martian meteorites is important.

Previous studies that investigated source rocks of the Martian meteorites have only targeted large (>10 km) and rayed craters on the surface of the planet (Mouginis-Mark et al. 1992; Tornabene et al. 2006; Hargitai and Kereszturi 2015), such as the Zunil crater in Cerberus plains (McEwen et al. 2005). An elliptical crater in the Syrtis Major region was suggested by Harvey and Hamilton (2005), as a source for the Nakhlite/Chassigny meteorites based on analysis of mineralogical information and age correlation. The 55 km Mojave crater was also suggested to be the source of shergottites by Werner et al. (2014a, b), although there is still an ongoing debate regarding this crater as a candidate source. The connection however between Mojave crater and shergottites is problematic as the crust there seems to be much older than the shergottite meteorites. For the NWA 7533 Martian meteorite the 6.9 km diameter, ~5 Ma old Gratteri crater (Wittmann et al. 2015) was proposed as a source.

Mineralogical, petrological, and textural properties of nakhlites, as well as evidence provided by secondary alteration, show that all these meteorites came from the same source rock unit (Changela and Bridges 2011). This evidence strongly suggests that the bolide impact ejected the nakhlites from a differentiated thick basaltic lava flow or a shallow sub-volcanic intrusion (Treiman 1993; Lentz et al. 2001). The solidification of the basaltic parent material occurred at about 1.2–1.4 Ga ago (Ganapathy and Anders 1969; Nyquist et al. 2001; Park et al. 2009; Cassata et al. 2010; Korochantseva et al. 2011), thus the source crater should be located in terrains of this age (estimated by crater-counting on Mars). Moreover, the ejection event occurred about 11 Ma ago, thus, the nakhlite source crater has to be of this age. These constraints a larger frame in which detailed investigations are performed in this study.

The current work adds to past efforts by investigating all craters with diameters above 3 km at lava plains with the corresponding formation age around 1.2–1.4 Ga. We have decided to include craters <10 km in diameter because computer simulations (Head et al. 2002), have shown that bolide impacts that produced craters with diameters down to 3 km on homogeneous and layered Martian terrains could have launched ejecta that escaped Martian gravitational field.

Spectral Properties of Meteorites and the Martian Surface

Spectral comparison of remote based Martian surface data and laboratory based data of Martian meteorites also provide input for source crater identification. Corresponding results are listed below according to meteorites. Analyzing the general spectral properties of meteorites and Martian lava flows, the composition of basalts in the Tharsis region somewhat resembles those of SNC's, especially shergottites, however no good match was found (Lang et al. 2009). The work of Ody et al. (2015) compared Los Angeles, Shergotty, QUE 94201, the lherzolitic shergottite ALH A77005, Nakhla, Chassigny and the orthopyroxenite ALH 84001 to the NIR data of the Mars Express OMEGA detector. The results suggest basaltic shergottites are similar in NIR spectral properties to early Hesperian volcanic provinces (Ody et al. 2015). Spectral resemblance between ALH 77005 and the Martian surface is poor, mainly its spectra similar to olivine-bearing regions like Nili Fossae and Noachian/early Hesperian terrains. For Chassigny similarities to spectra from the Nili Patera caldera was identified, while for ALH 84001 areal analogies exist at northeast of Syrtis Major and northwest of Hellas basin, regarding the low-calcium-pyroxene-rich composition and old age (but not for the modal mineralogy). Unfortunately no convincing spectral analogue was found for the Amazonian-aged Nakhla

meteorite. It is generally expected that dust cover significantly influences the remotely acquired spectra (Ody et al. 2015) and makes possible identification difficult.

Non SNC member NWA 7034, 7533 and 7455 Martian brecciated meteorites showed spectral signatures consistent with a near surface Noachian aged terrain. Among them NWA 7533 do not show strong mafic mineral absorptions, but is consistent with a large part of the Martian highlands' spectra (Beck et al. 2015). Besides classical spectral analysis, gamma-ray spectroscopy could also be used to compare meteorite and Martian surface composition. In the case of NWA 7475 the comparison to gamma-ray spectrometer results onboard Mars Odyssey shows that the Fe and Ti abundances are compatible with the composition of the estimated average southern highlands in general. At this area a possible source crater was also identified: the 6.9 km diameter Gratteri crater, aged about 5 Ma old (Wittmann et al. 2015).

A recent fall, the Tissint meteorite (Chennaoui et al. 2012), shows petrographical similarities to shergotites. Its powder measured with visible and near infrared spectrometer were compared to CRISM based spectra of the pyroxene and melt rich outcrop of Alga crater on the Martian surface (Mustard et al. 2013).

Characteristics of Nakhlites

Analysis of nakhlite meteorites suggests that the target area on the Martian surface requires a basaltic substrate, which is iron rich and aluminium poor (Treiman1993; Treiman 2005). Mineralogically clinopyroxene is the most abundant mineral in nakhlites (70–80 vol%), the second most common is olivine (9–12 vol%), while there are also feldspars and some refractory minerals in the mesostasis (8–11 vol%, or up to 20 vol% in NWA nakhlites, Treiman 2005). Their cumulate texture suggests that the parent rock of the nakhlites was formed by slow cooling below the surface (Treiman2005); however, the mesostasis is composed of fine-grained material which indicates faster cooling, similar to those close to the surface of a lava flow. The distribution of trace and minor elements in augites suggests that Nakhla, Governador Valadares, Lafayette, Y000593 (Mikouchi et al. 2003) and some other nakhlites (Corrigan et al. 2013) might be samples from different horizons of the same lithologic unit (Wadhwa and Crozaz 1995), although late magmatic and subsolidus diffusion might cause changes to this primary zoning (Harvey and McSween 1992). Similarly, the degree of alteration of the different nakhlites is interpreted to provide evidence for their origin from different horizons of the same parent rock (Changela and Bridges 2011).

Microphotographs of the major secondary mineral assemblages found in Nakhla are shown in Fig. 1 (Chatzitheodoridis and Turner 1990; Chatzitheodoridis et al. 2014). Alteration minerals include evaporitic assemblages such as carbonates, sulfates, and halides (Chatzitheodoridis and Turner 1990; Gooding et al. 1991; Bridges and Grady 1999, 2000; Chatzitheodoridis et al. 2014), hydrous minerals such as iron-rich silicate rust (probably smectite, Gooding et al. 1991) and clays (Changela and Bridges 2011; Chatzitheodoridis et al. 2014), and finally, hematite and marcasite (Chatzitheodoridis et al. 2014). All alteration is pre-terrestrial and formed by moderate to very low temperature olivine-water interaction, where water is either igneous in origin or produced by melting of ice from the permafrost (Karlsson et al. 1992; Chatzitheodoridis et al. 2014). Alteration minerals are important because they indicate that the rock of the nakhlites has undergone at least two alteration events. Alteration was initiated by hydrothermal fluids (about 913 Ma ago), which locally melted the parent rock and reset the age according from radiogenic isotopes (Cassata et al. 2010), and which might have formed rhoenite and Al-rich clinopyroxene

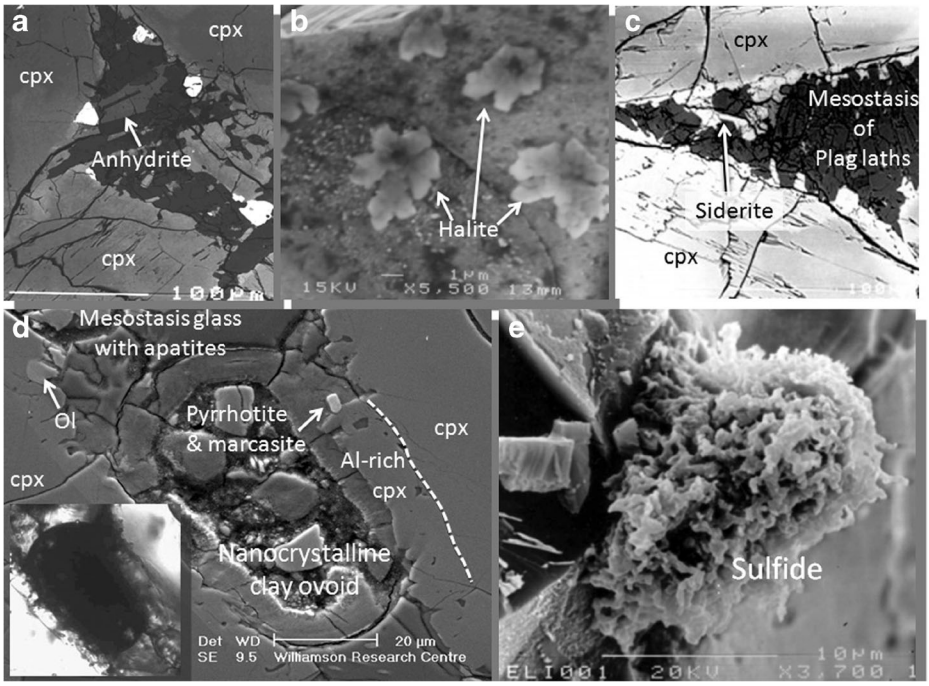

Fig. 1 Examples of secondary minerals in Nakhla made with the electron microscope from thin sections (backscattered images **a**, **c**, and **d**), or from pristine surfaces of Nakhla grains (secondary electron images **b** and **e**). **a** Sulphate crystal (anhydrite) in mesostasis. **b** A leaf-shaped halite, grown on a pristine clinopyroxene surface from a freshly opened, untreated Nakhla grain, most probably of Martian origin. **c** The first reported siderite in a Nakhla mesostasis (Chatzitheodoridis and Turner 1990). **d** Ovoid in Nakhla mesostasis, made of nanocrystalline clay (reproduced image from Chatzitheodoridis et al. 2014) and various minerals, such as cumulus clinopyroxene crystals (cpx) with Al-rich rims, olivine (Ol), a pyrrhotite grain altered to marcasite, and acicular apatite crystals in mesostasis glass. The inset image in (**d**) is the ovoid shown under the transmitted optical microscope. **e** A sulfide grain grown on a pristine clinopyroxene grain from an untreated, freshly opened Nakhla grain, therefore most probably of Martian origin

rims in Nakhla (Chatzitheodoridis et al. 2014). The second impact ejected nakhlites at 11 Ma ago (Ganapathy and Anders 1969; Eugster et al. 2002).

In summary, it is expected that the source crater from which the nakhlites have been ejected was formed on a lava plain. Lithologies from vertical strata up to several tens of meters depth were extracted, which contain both slow-cooled subsurface cumulus rock units and fast-cooled near-surface rock units. Overprinted alterations might have been potentially formed by a previous impact that caused partial melting and initiated hydrothermal systems, before 11 Ma ago an impact finally ejected the meteorites. Water abundance in the area might have been too low to produce morphological surface manifestations at the lava flow, but it was enough in volume and time, to leave behind the strong alteration signatures that are observed in nakhlites.

Methods

We used remote sensing datasets from Mars to search for candidate source craters of the nakhlite meteorites. We surveyed all volcanic units dated to 2.1—0.3 Ga (Hartmann and Neukum 2001)

with the upper limit was between 2.1 and 1.4 and the lower limit at 0.6–0.3 because of uncertainties. These areas were outlined according to the mapped units based on the Geological map of Mars Map 3292 of scale 1:20,000,000 made by USGS (Tanaka et al. 2014), with overlying the borders of the corresponding aged surface areas with THEMIS image maps. Altogether 17.3 million km^2 area was surveyed. Those areas are indicated by a white outline in Fig. 6. The mapping procedure was to:

1. select areas that are covered with lavas 2.1–0.3 Ga old,
2. survey those areas both on daytime and night-time THEMIS mosaics looking for the rayed craters (Christensen et al. 2003, 2004) with detailed analysed the candidate craters using THEMIS and CTX (Malin et al. 2007) data. THEMIS dataset was selected as a main source of data in this study because it enables the firm identification of fresh craters with diameters down to the km size. The comparison of the daytime and nighttime IR images of Mars clearly shows the albedo contrast between the ejecta and the surrounding area (Tornabene et al. 2006). Additionally, THEMIS data provide almost continuous coverage of the planet, although—as it turned out during this analysis—not all probable recent craters showed rays both in infrared and optical images (Piatek et al. 2014). CTX dataset was too detailed for the analysis of relatively large craters and the survey of large area. This step was done using the JMARS software (Gorelick 2003),

Basic Constraints

Based on crystallization age constraints of nakhlite meteorites (1.24 Ga ±0.01 by Gale et al. 1975 or 1.28 Ga ±0.06 by Nakamura et al. 1977) and taking into account the uncertainty of the crater density based surface age estimation (Hartmann and Neukum 2001; Hartmann 2005) we used the extended time interval to 2.1–0.3 Ga for the selection of the surveyed surface area. (However, based on isotopic dating of hydrothermal alteration produced minerals in the meteorites, the area where the nakhlites were ejected has undergone at least two alteration events.) Although lava flows of Amazonian age also exist at the Hesperia volcanic province in the southern hemisphere of Mars, the youngest lava flow that is present there is about 2.2 Ga (Lehmann et al. 2012) which is significantly older than the age of nakhlites crystallization. Another small area of young lava flows exists in the Syrtis Major region with an age younger than 1.4 Ga (Jodlowski et al. 2013). These areas were not included in this study.

Constraints for the crater size are influenced by the mechanical strength of the targeted terrains; i.e., a porous terrain requires larger craters. Based on model computations of impact process and particle ejection, the source craters of the Martian meteorites have to be larger than 3 km in diameter (Head et al. 2002), while earlier studies suggested that 12 km is a minimal crater diameter (Melosh 1985). Specifically for Nakhla, some models calculate a minimum of 15 km diameter (Warren 1994). In this survey of rayed craters on young Amazonian lava plains we have included craters from 0.5 km up to 100 km in diameter, to see how our findings fit to the expected crater production rate, and such comparison is more relevant if a wider range of crater size was taken into account.

The third requirement is the meteorite ejection age (source crater age) of about 11 Ma. Young craters are usually identified based on their pristine appearance and existence of easily erodible ejecta, i.e., features such as rays (Hawke et al. 2004), and containing few or no overprinting of small craters (Boyce and Garbeil 2007).

Context for the Potential Nakhla Target Crater

From the ejection age of Nakhla, the target crater should have formed at around 11 Ma ago, and the area where it is located should form around 1.2 Ga. It is therefore worth searching areas with a spatial density of craters indicating such an age. Figure 2 shows a crater size-frequency distribution diagram with isochrones (after Hartmann and Neukum 2001) to visualize the expected areal density of potential source crater. The candidate craters should show a population of superimposed craters following the 11 Ma. The spatial density of km sized craters (horizontal axis) should be about 10^{-6}–10^{-7}craters/km^2. This confirms that within reasonable limits our methodology is valid. However, a few larger craters launched most ejecta (Gladman 1997), thus the best candidate craters should be the larger ones.

Results

This section outlines the basic constrains of the survey, e.g., where the survey was realized and what type of craters we searched for. The identified rayed craters are listed in Table 1. Based on this, general and specific cases, including the best candidates, will be presented in the discussion.

The characteristic appearance of fresh craters targeted this study are shown in Fig. 3. A recently formed large crater is Mojave crater (327.0E 78.5 N), its age is estimated to be from 2 to 10 Ma old (age estimation was based on the craters' spatial density on its ejecta; Werner et al. 2014a, b Fig. 3a, d). This 55–60 km diameter crater retained its ray system (Werner et al. 2014a, b). Several smaller craters in this area appeared very recently, i.e. during the time were images of Mars were recorded (Dauber et al. 2013). These very recent craters are not indicated in Fig. 3 as we only look for larger, km scale craters. Zunil crater (143.5E 7.4 N; Fig. 3b, e,

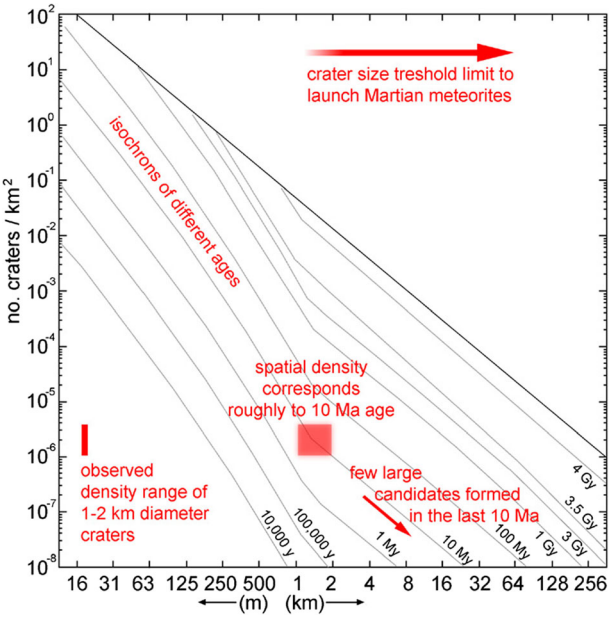

Fig. 2 Crater size frequency distribution diagram displaying the expected areal occurrence of identified rayed craters (Table 1) craters (square in the centre) with threshold limit (the 3 km) to launch projectiles on interplanetary orbit, and other parameters (indicated as an arrow points to the right at the top of the diagram)

Table 1 List of rayed craters identified within lava surfaces dated to (2.1–0.3Ga) in the Elysium and Tharsis regions. The appearance on daytime and nighttime THEMIS images was characterized by numbers between 0 and 3 (0:no rays or halo, 1:weak rays or weak halo, 2:>4 distinct rays, 3:>10 separated rays)

Longitude (east)	Latitude (north)	Diameter (km)	Daytime appearance	Nighttime appearance
118.014	29.344	2.4	2	2
184.49	43.086	3.3	3	1
118.848	44.289	1.4	1	1
121.555	29.004	4.5	2	2
122.242	23.971	10.9	1	0
124.084	27.031	4.7	1	2
126.057	20.154	12.6	1	0
128.199	35.539	5.2	1	1
128.717	26.346	3.7	0	1
129.561	26.986	6.2	0	1
130.176	29.186	1.8	1	1
130.799	29.674	6.5	0	1
131.494	19.477	1.1	1	2
134.176	24.844	3.8	1	1
135.023	8.387	1.6	2	2
136.986	8.402	1.8	3	2
138.213	4.588	2	2	2
148.309	0.533	4.6	2	2
151.801	10.986	2.4	2	2
152.678	10.285	0.7	1	1
154.951	9.09	1.2	1	0
158.996	4.686	2.2		
159.187	15.512	1.3	3	3
206.49	50.58	1.3	1	3
225.346	54.465	1.3	3	1
226.621	54.469	2.3	3	3
229.459	47.463	0.7	1	1
236.275	60.289	3.3	3	no data
237.426	65.244	0.9	3	no data
237.848	58.131	0.6	0	1
238.242	56.775	1.4	2	0
240.445	55.418	0.6	3	0
241.182	66.01	0.9	3	no data
243.355	31.262	14.6	2	0
243.771	60.639	0.6	3	no data
243.771	60.639	0.4	2	no data
246.434	16.969	0.3	3	0
247.656	63.567	2.1	2	no data
247.844	47.686	7.2	2	1
250.711	55.451	0.5	3	0
251.256	65.33	0.5	1	no data
251.992	53.729	1.5	3	0

Table 1 (continued)

Longitude (east)	Latitude (north)	Diameter (km)	Daytime appearance	Nighttime appearance
253.285	58.055	0.7	3	0
253.312	49.57	0.4	1	0
254.137	52.885	0.6	3	0
255.682	44.533	2.1	1	0
255.717	51.889	2.9	2	1
257.521	64.506	1.1	2	0
259.174	47.314	0.9	1	0
259.105	65.355	1.7	3	no data
263.553	47.336	1	3	0
265.365	52.799	1.1	1	1
267.494	53.467	1.6	1	1

McEwen et al. 2005) is also a relatively young (1.5–2.7 Ma) and large (10 km diameter) crater with a ray system, although less prominent than that of the Mojave crater (Preblich et al. 2007).

Craters that are formed during the acquisition of images from the Martian terrain can provide a good tool to estimate the impact rate, especially when it is combined with information on the erasing rates of the dark rays (Geissler et al. 2010). A good example can be found at the coordinates 246.434E, 16.969 (Fig. 3c, f), of which a detailed view is on the HiRISE PSP_002183_1970 image (Morgan and Murchie 2013). It shows radial rays only in

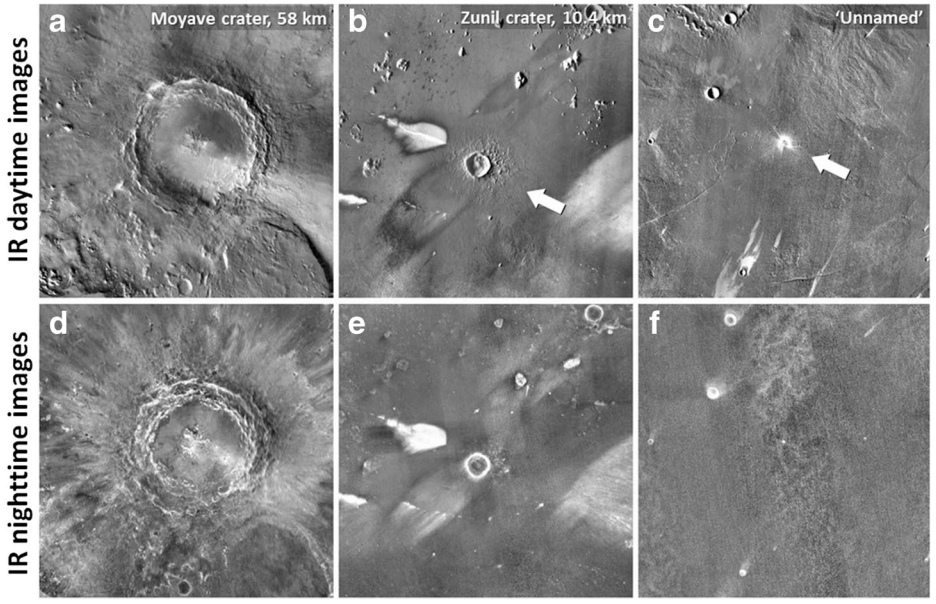

Fig. 3 Example THEMIS IR daytime (top) and nighttime (bottom) images of three recently formed craters: (**a**, **d**) Mojave crater (58 km); (**b**, **e**) Zunil crater (10.4 km); and (**c**, **f**) an 'unnamed' very young small crater (about 2 km). Note that the young ejecta and rays cannot be observed in every case both on daytime and nighttime images. The craters sought in this work are larger than the 'unnamed' one of this figure. For comparison, all images are extracted from JMARS with the same pixel resolution. (THEMIS images are from the Planetary Data System)

the daytime IR image of the THEMIS detector (Fig. 3c). As in many cases, also in this example fresh impact craters are not erased by global dust storms for several years.

Ray Identification and Usage

Two important questions and issues regarding the rayed craters on Mars are their retention age, and the identification of crater rays. While obvious ray systems for km sized craters are relatively rare in the visual part of the spectrum (Tornabene 2005), using THEMIS images and careful inspection, a reasonable number of them could be identified especially in the small size range (McEwen et al. 2005). However there is an ongoing debate on which features should be classified as rays: the case of the largest ones is mostly evident, but it is more difficult to classify the smaller and less pronounced ones, especially as erosional agents make them fading with time. At certain locations rays could show specific appearance and regionally elevated concentration on infrared images like at the Cerberus region where many small (100–200 m) bright-rayed craters are observed (McEwen et al. 2005) beside the large ones (Malin et al. 2006). In this work we searched for candidate source craters that impact ejected the nakhlite meteorites, and listed craters including those with the less pronounced ray systems. The reason for this strategy is that most probably at certain regions rays are fading away faster (see the Discussion for the inhomogeneous spatial distribution of rayed craters).

In this work we add an effort to identify the features that appear as several radially elongated albedo stripes beyond the ejecta blanket (Hartmann et al. 2010). We noted great differences between certain ray systems (see Fig. 4). Although these central craters do not exhibit obvious rays, the rays are still observable (probably somewhat older than their more obvious counterparts), thus they also need to be considered during the analysis. Such candidate craters with less obvious ray system should require more detailed analysis with higher resolution images – that could be a next step after this research.

Based on image analysis performed in this work, daytime IR images show the fresh ray system more frequently than the nighttime IR images. This is a good indicator of the young age, using the albedo contrast of the ejecta rays to reveal subsurface material, with the high albedo contrast both in the optical and the infrared region (Morgan and Murchie 2013). There is also a possible age and climate related connection that explains the relatively young ejection age of Martian meteorites. Based on Fritz et al. (2007) model, surface regions not covered with ice were especially favoured for impact ejection of the past ~ 5 Myr after the last major glaciations on Mars (Fritz et al. 2007; Schon and Head 2012). A fraction of the impacted body's energy is released in this upper icy unit. As impact ejects part of the topmost unit of the surface layer to interplanetary orbit, and if m thick ice-dust layer covers it, the fraction of the ejected part from this unit because its fragility and volatile content probably cannot recovered as meteorites on the Earth or other planetary body, decreasing the probability of having meteorites from ice covered area on Mars.

Candidate Craters

Table 1 describes the characteristics of those rayed craters that were identified during this survey. Here craters below 3 km diameter are also indicated to provide possibility to analyze their size frequency distribution in a wider range and fit to the model based expectations. The best candidates are larger than 3 km, are sharp-edged craters displaying obvious ray systems, both in the daytime and the nighttime images. Craters smaller than 3 km are indicated here,

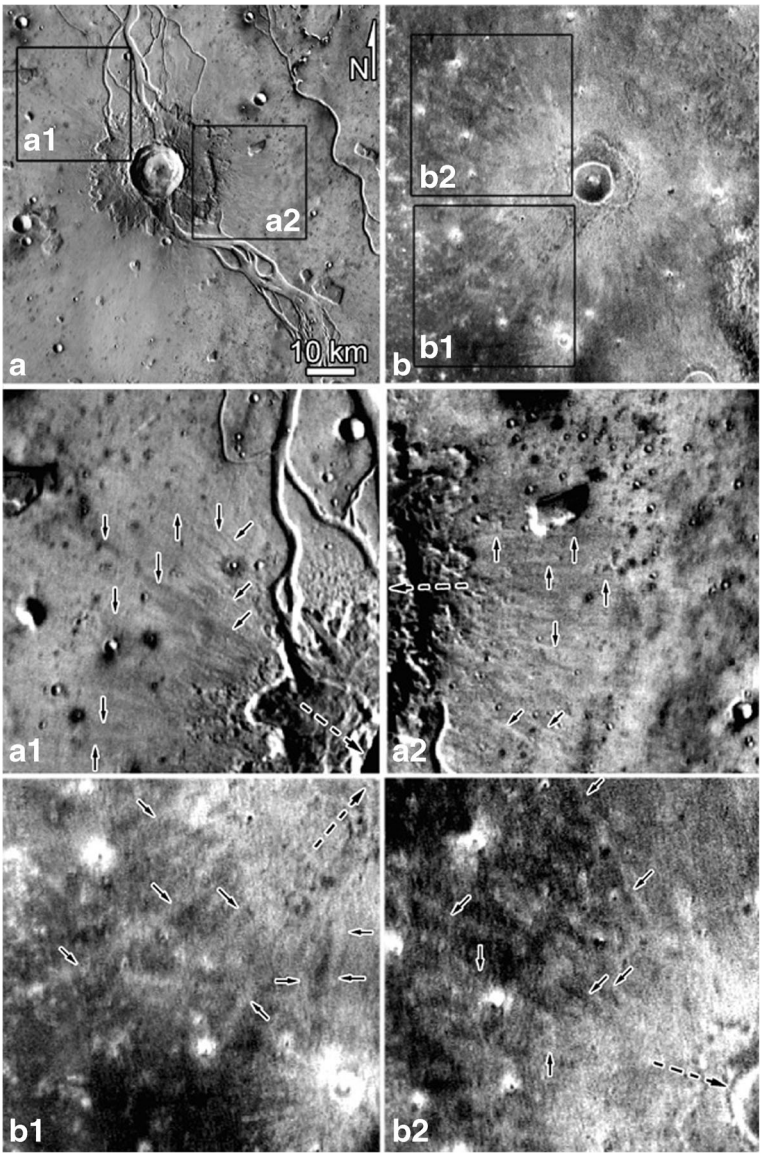

Fig. 4 Two examples for the observable, although not obvious crater rays for two pedestal craters on optical (a, a1, a2) and infrared (b, b1, b2) THEMIS images. Inserts a1, a2, b1, b2 show magnified versions of locations indicated by boxes in *a* and *b* insets. *Small arrows* mark the radial streaks that form ray-like features occasionally to several crater radii from the central crater, the *longer dashed arrows* point to the direction of the central crater (which are outside the inset images' area)

despite they are not likely candidates. Their distribution and characteristics however could be used as indicators for the general properties of recent impact scars on Mars.

A selection of interesting, but less "regular" craters is displayed in Fig. 5a–c. They show unusual "rays" as overprinted elongated topographic anomalies in addition to structures of different albedo. These "rays" are not real ejecta rays, but topographic structures that probably

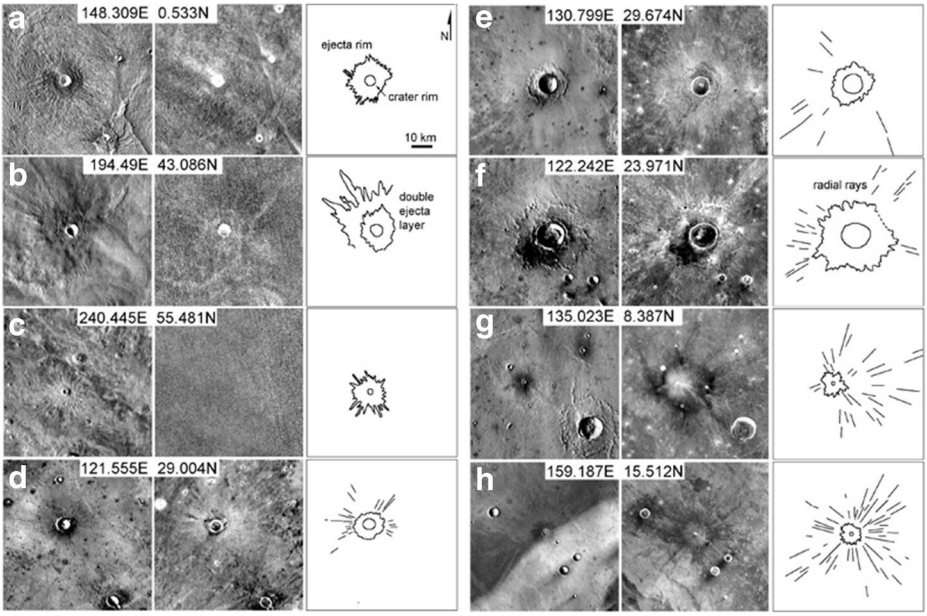

Fig. 5 Daytime (1, 4 columns) and nighttime (2, 5 columns) THEMIS image pairs of craters, and their morphological outline (3, 6 columns). These craters present characteristic features considered during this work. (**a–c**) Craters with ray like elongated parts of the ejecta blanket, formed by old remnants left behind selective erosion (see the text for details). (**d–f**) Craters with faint rays beyond a thick proximal (**d**) and fluidized ejecta blanket (**e**, **f**). (**g–h**) Examples of more abundant ray systems with various morphologies (for even higher resolution versions see also Fig. 4). (THEMIS images are from the Planetary Data System)

formed by selective erosion of material surrounding the crater, structures more resistant to erosion is shielding the material underneath and leaves behind raised platforms. The cemented/hardened nature of these rays can be seen in the nighttime images, where ejecta rays are almost invisible (except the craters on Fig. 5b, c). Such structures characteristics of older craters, and thus are not relevant candidates, thus were not included in the table.

Few pedestal craters also show weak rays (Fig. 5e, f) extending beyond the edge of the fluidized ejecta blanket. These craters are important targets for further analysis as they might hint to ice stored in the subsurface that produced the fluidized ejecta blanket.

The spatial distribution of the 53 identified candidate craters is visualized in Fig. 6. During the survey, 23 rayed craters were identified at the Elysium area (surveyed an area covering 3,505,573 km^2) with areal density of 6×10^{-6} craters/km^2, and 30 craters at the Tharsis region (at 13,857,576 km^2 area) with 2×10^{-6} craters/km^2.

Discussion

Analysing the sizes of the identified young candidate craters, a roughly exponential increase from smaller to larger craters is present, with more craters of smaller diameters (Fig. 7). The identified craters are 0.5–15 km in diameter. The theoretical size-distribution model curve for 11 Ma aged craters (Hartmann and Neukum (2001) is also indicated with grey colour (grey solid line), calculating with spatial crater density (grey logarithmic axis at left) for the total surveyed 17.3 million km^2. The observed size frequency distribution is in good agreement

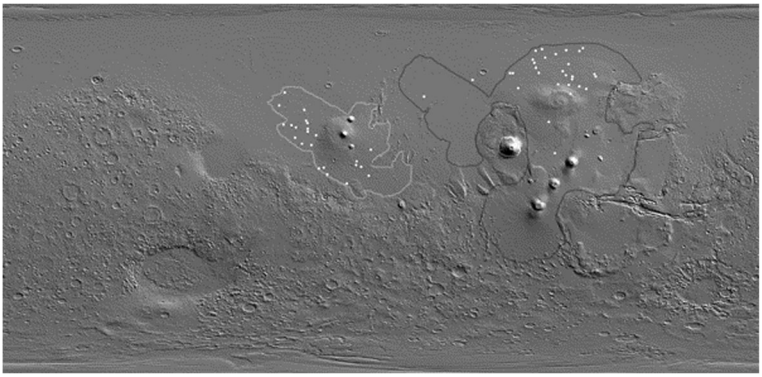

Fig. 6 Spatial distribution of identified rayed craters on a MOLA shaded topographic map in Mercator projection. The *gray lines* shows the edges of the analysed young lava plains at Elysium (*gray line*) and Tharsis (*black line*) while the *white dots* show the locations of candidate craters

with the expectations regarding the trend – although the craters are a bit smaller in number, possibly because of some process that removed or less preserved craters at certain locations.

Most of these young structures (left part of the diagram in Fig. 7) fall below the crater size required to launch substantial mass that escapes Mars, but these smaller craters suggesting that the selection of young craters used in this work was relatively effective. The diagram also shows the theoretical size-frequency distribution of small craters formed in the last 11 million years using data from Hartmann and Neukum (2001).

In theory the craters should be distributed homogeneously, but at the southern and western part of the Tharsis area only few candidates were identified. The lack of young candidate craters in these areas might be connected to the topography (elevation and/or slopes). For example, the rayed craters of the Elysium region are located below −1200 m topographic height; in the Tharsis region they are mostly below −1000 m (except of two cases that are at

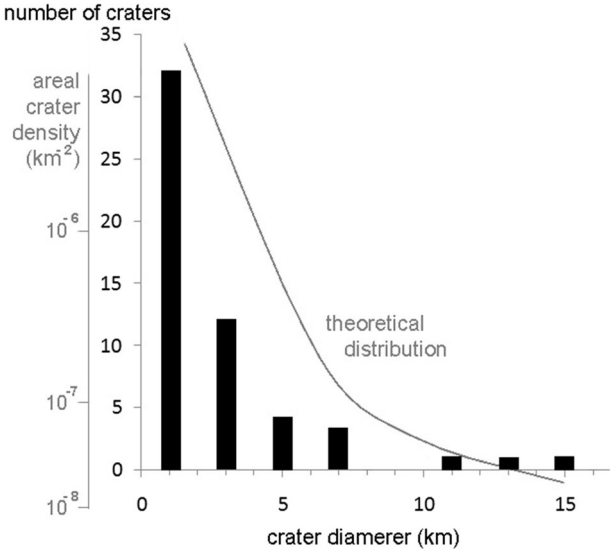

Fig. 7 Size frequency distribution of the identified craters grouped by 2 km diameter bins

the elevation of +2200 m). Rayed craters exist on airless bodies too, thus the rare atmosphere need not necessary produce absence of rays on Mars; however, the difference in air density might have an effect on ray formation or retention on Mars, and it is also possible that strong slope winds are present at the steep slopes of Tharsis (Magalhaes and Gierasch 1982) and could have erased them quickly. But other possibilities also exist, thus more detailed work is required for the exact analysis of this issue that should be the topic of another work.

The Best Candidates

From the list of all rayed impact craters identified on roughly Middle Amazonian aged volcanic units (see the outline of the surveyed areas in Fig. 8), we have selected craters that seem to be the best candidate sources crater of the nakhla meteorites (Table 2). These craters show a ray system both on daytime and nighttime THEMIS images, and they have diameters above 3 km. The largest rayed craters on the lava terrains of appropriate age are shown in Fig. 7 on daytime (left) and nighttime (right) images. A critical point here is the firm identification of ray systems, as they show quite a wide range of appearances. For example the ray system in the case of the a1-a2 crater was less evident (faint and scattered rays with low spatial density), and in the case of the d1-d2 crater the rays show only a moderate density and one of them shows an unusual curved shape.

All of the candidate craters are located at relatively smooth lava plains, without signs of significant vertical lava mixing (like large tilted, chaotic lava blocks or small cones), suggesting rock units originally crystallized at the bottom or top of the lava flow could not have

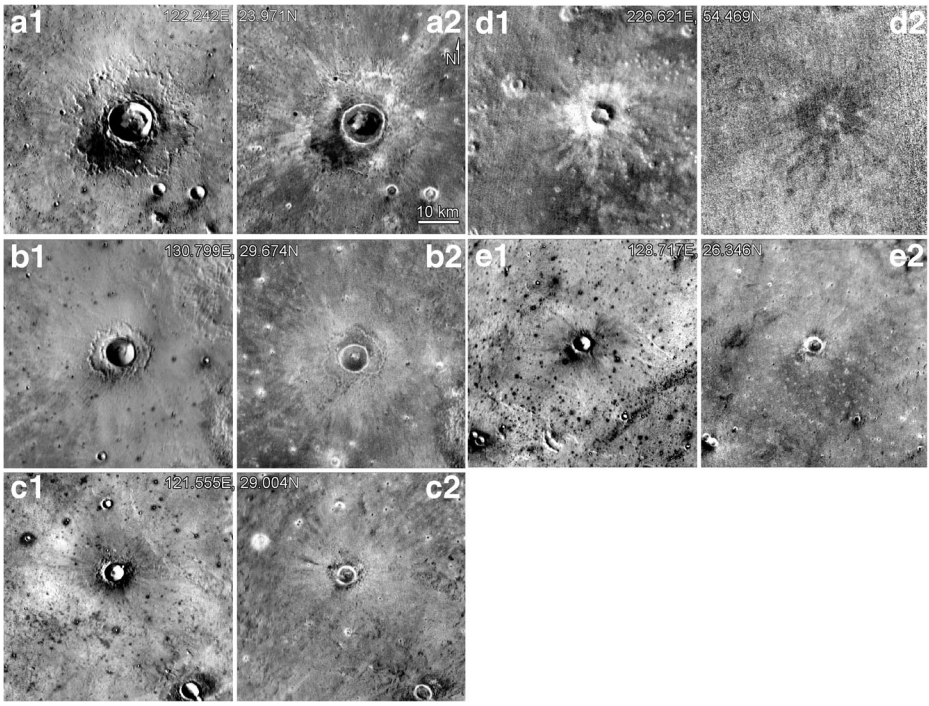

Fig. 8 Image mosaic of the best candidate craters on daytime (a1, b1, c1...) and nighttime (a2, b2, c2...) THEMIS images. *Arrows* mark those rays, which are difficult to identify otherwise

Table 2 Characteristics of the best candidate craters listed according to decreasing size order

Coordinate (inset Fig. 8)	Diameter (km)	Crater rays' appearance	Surface H_2O sign	Subsurface H_2O sign	Characteristics of the area
126.057E, 20.154 N	12.6	Poor, only in IR, could be older than 11 Ma	Dendritic valley there	Fluidized ejecta lobe	Smooth lava surface
122.242E, 23.971 N (a)	10.9	Poor, mainly only in IR, could be older than 11 Ma	-	Fluidized ejecta lobe	Smooth lava surface
130.799E, 29.674 N (b)	6.5	Poor, mainly in IR, could be older than 11 Ma	Possible valleys nearby	Fluidized ejecta lobe	Lava or water channels
121.555E, 29.004 N (c)	4.5	Developed ray system	-	-	Few lava flow lobes
128.717E, 26.346 N (e)	3.7	Moderately developed rays	-	-	Relatively smooth lava plain
226.621E, 54.469 N (d)	2.3	Developed ray system, but too small	Uncertain nearby valley	-	Few lava flow lobes

brought closer to each other, as it is observed in the nakhlites' mineral pattern; although, small scale vertical mixing could easily take place during the horizontal movement of the lava flow without observable surface manifestation. In three cases (see them in Table 2) several cases, the candidate craters show fluidized ejecta blankets and valleys, which are suggestive of subsurface water or ice —it is however not possible to know whether this H_2O was present there during the cooling of lava, or came later as ice precipitation on the surface.

An important consideration is also the depth of excavation during a meteor impact, which increases from 0.25 km to about 1 km when the diameter of the crater increases from 1 to 10 km (Tornabene et al. 2013). Numerical simulations suggest that for material that reaches the Martian escape velocity the depth of origin is ~10 % of the impactor's diameter (Artemieva and Ivanov 2004).

The best candidates for source craters are listed in Table 2. It is difficult to select one ideal crater among them for this purpose, as the larger ones show quite poor and faint rays around them, although signatures for the presence of subsurface H_2O exist there, which is compatible with the water related alterations in the nakhlite meteorites. Craters with more pronounced ray systems are smaller, around the threshold limit of 3 km diameter, with moderate chance to launch rocks to heliocentric orbit. The survey in this work points to several questions where more focused research is required to consider potential source craters of nakhlites, i.e. the evaluation of ray systems with different level of appearance, and the ranking of effects and their consequences that erase ray systems.

During this work several difficulties emerged to identify rayed craters, especially if they are heavily eroded and/or relatively old. Bright or dark halos can occasionally look somewhat similar to the proximal part of coalescing rays — their separation from real rays requires careful analysis. Halos might occasionally form by the wind activity (forming by small patches that might look like a halo, close to the limit of the resolution, but not radial elongated streaks). They can also form by the exhumation of different materials that are not visible on the surface,

and the search for elongated rays requires special care. The quality of images significantly influences the investigation, and it is getting more difficult towards higher latitudes where data are scarce. In some cases, older ray-bearing craters might have been misidentified as fresh ones, since these rays are not only albedo features but also the result of selective erosion that enhances the system of radial ridges (i.e. Fig. 5a, b, c) – but careful analysis helps here much.

Cases, where large ray system does not exists, while some radial albedo features are still present beyond the edge of the ejecta are difficult to interpret. These might be older and degraded systems of formerly existing well-developed rays. In these cases the age constrain might not work well. The inhomogeneous areal distribution of the identified craters suggests that on Mars erosion acts in different intensity at surfaces of different altitude, thus producing eroded ray systems with different appearance. This makes the definition and use of age constrains uncertainty, and more focused analysis is necessary.

Conclusion

We have surveyed an area of 17.3 million km^2 of about 1.2 Ga old Martian lava terrains, an age that is corresponding to the crystallization age of the nakhlites, to search for craters with rays that are probably young, similar to the ejection age of the nakhlites about 11 Ma. Altogether, 53 rayed craters within late amazoninan aged lava flows were identified. However, most of them are too small (between 1 and 3 km diameter) to match all required criteria. The methodology of using the associated ray system as an indicator for a young age seems to work well, because the measured areal density of craters around 10^{-6} km^{-2} agrees will with the number of craters predicted by recent bombardment rate models. A profound uncertainty of the analyses of the remote sensing data is the absence of about 1/3 of potential candidates, which might be located on terrains with a high topographic elevation or on surfaces of steep slopes – but the exact role of such terrains on the appearance of crater rays require more work beyond the scope of this paper. These regions display an apparent deficit of rayed craters, suggesting that the ray retention could be influenced by slope winds (strong katabatic winds with daily cycle, caused by the high daily temperature and pressure change especially along slopes of large topographic undulation (Kite et al. 2013) above the generally low thermal inertia Martian surface). A detailed analysis of this possibility is beyond the scope of this paper.

From the 53 rayed craters on corresponding age lava terrains that were identified in this study, only about a dozen can be considered as actual candidates. They are all above 3 km in diameter what means they have sufficient size to launch a meteorite on the heliocentric orbit, with Earth as their final destination. Roughly half of the best candidates are located close to possible fluvial valleys, while only three of them show a fluidized ejecta blanket. The latter implies the presence of subsurface water ice, but in these cases the rays are poorly developed, and probably they are older craters, not satisfying the constrain for a young age. Here the poor, fragmented ray system requires improved interpretation for age estimation. Water is a strong indicator for a nakhlite parent rock, since all nakhlites are hydrothermally altered, or contain secondary minerals that imply hydrous activity. We already have certain geochemical, mineralogical, and petrological information from the nakhlites that could be matched with existing remote sensing data but possibilities will improve in the future with improved and more detailed remote studies. More detailed studies could, especially focusing on chemical and mineralogical information, similar to those mentioned in section 3.1 (“Basic constrains”) could

help to narrow the list of candidate craters. An effort should also be made to locate those candidate craters that are not identified with the current methodology due to the lack of (probably eroded) ray systems. This effort however requires a better understanding, which features shall we classify as a ray system and how do they form. The reason is that ray systems cannot be easily classified because variable methods of erosion influenced their appearance to different degrees and on different terrains.

Acknowledgments This work was supported by the COST TD 1308 project, the OTKA 105970 and NKFIH COOP K 119372 funds. The authors also acknowledge the critical comments from the referees that supported to improve the work substantially.

References

Artemieva NA, Ivanov B (2004) Launch of martian meteorites in oblique impacts. Icarus 171:84–101
Beck P et al. (2015) A Noachian source region for the "Black Beauty" meteorite, and a source lithology for Mars surface hydrated dust? EPSL 427:104–111
Boyce JM, Garbeil H (2007) Geometric relationships of pristine Martian complex impact craters, and their implications to Mars geologic history. GRL 34. doi:10.1029/2007GL03931
Bridges JC, Grady MM (1999) A halite-siderite-anhydrite-chlorapatite assemblage in Nakhla: mineralogical evidence for evaporites on Mars. MAPS 34:407–415
Bridges JC, Grady MM (2000) Evaporite mineral assemblages in the nakhlite (Martian) meteorites. EPSL 176: 267–279
Cassata WS et al. (2010) Evidence for shock heating and constraints on Martian surface temperatures revealed by $^{40}Ar/^{39}Ar$ thermochronometry of Martian meteorites. GCA 74:6900–6920
Changela HG, Bridges JC (2011) Alteration assemblages in the nakhlites: variation with depth on Mars. MAPS 45:1847–1867
Chatzitheodoridis E, Turner G (1990) Secondary minerals in the Nakhla meteorite. MAPS 25:354
Chatzitheodoridis E et al. (2014) A conspicuous clay ovoid in Nakhla: evidence for subsurface hydrothermal alteration on Mars with implications for astrobiology. Astrobiology 14:651–693
Chennaoui A et al. (2012) Tissint Martian Meteorite: A Fresh Look at the Interior, Surface, and Atmosphere of Mars. Science 338:785–788
Christensen P et al. (2003) Morphology and composition of the surface of Mars: Mars Odyssey THEMIS results. Science 300:2056–2061
Christensen P et al. (2004) The Thermal Emission Imaging System (THEMIS) for the Mars 2001 Odyssey Mission. SSR 110:85–130
Corrigan CM, Velbel MA, Vicenzi EP, Konicek A (2013) Nakhlite NWA 5790: Modal mineralogy and comparison with the rest of the nakhlites. Meteorit Planet Sci 48:A5309
Dauber et al. (2013) The current Martian cratering rate. Icarus 225:506–516
Eugster O et al. (2002) Ejection ages from krypton-81-krypton-83 dating and pre-atmospheric sizes of Martian meteorites. MAPS 37:1345–1360
Fritz J et al. (2007) The Martian meteorite paradox: Climatic influence on impact ejection from Mars? EPSL 256: 55–60
Gale NH et al. (1975) The chronology of the Nakhla achondrite meteorite. EPSL 26(2):195–206
Ganapathy R, Anders E (1969) Ages of calcium-rich achondrites—II: Howardites, nakhlites, and the Angra dos Reis angrite. GCA 33:775–787
Geissler PE et al. (2010) Aeolian degradation of young Martian craters. 41st LPSC, 2591
Gladman B (1997) Destination: Earth. Martian meteorite delivery. Icarus 130:228–246
Gooding JL et al. (1991) Aqueous alteration of the Nakhla meteorite. Meteoritics 26:135–143
Gorelick NS (2003) JMARS: A Multimission Data Fusion Application. 34th LPSC, 2057
Hargitai H, Kereszturi A (2015) Crater ray. In: Encyclopaedia of planetary landforms. Springer, New York Heidelberg Dordrecht London
Hartmann WK (2005) Martian cratering 8: Isochron refinement and the chronology of Mars. Icarus 174:294–320
Hartmann WK, Neukum G (2001) Cratering chronology and the evolution of Mars. SSR 96:165–194
Hartmann WK et al. (2010) Do young martian ray craters have ages consistent with the crater count system? Icarus 208:621–635

Harvey RP, Hamilton VE (2005) Syrtis Major as the Source Region of the Nakhlite/Chassigny Group of Martian Meteorites: Implications for the Geological History of Mars. 36th LPSC, 1019
Harvey RP, McSween HY (1992) Petrogenesis of the nakhlite meteorites - Evidence from cumulate mineral zoning. GCA 56:1655–1663
Hawke BR et al. (2004) The origin of lunar crater rays. Icarus 170:1–16
Head JN et al. (2002) Martian meteorite launch: high-speed ejecta from small craters. Science 298:1752–1756
Jodlowski P et al. (2013) Eruption history of the Syrtis Major Volcanic Province, Mars. 44th LPSC, 2322
Karlsson HR et al. (1992) Water in SNC meteorites - Evidence for a Martian hydrosphere. Science 255:1409–1411
Kite ES, Lewis KW, Lamb MP, Newman CE, Richardson MI (2013) Growth and form of the mound in Gale Crater, Mars: Slope wind enhanced erosion and transport. Geology 4:543–546
Korochantseva EV et al. (2011) ^{40}Ar-^{39}Ar and cosmic-ray exposure ages of nakhlites—Nakhla, Lafayette, Governador Valadares—and Chassigny. MAPS 46:1397–1417
Lang NP et al. (2009) Tharsis-sourced relatively dust-free lavas and their possible relationship to Martian meteorites. JVGR 185:103–115
Lehmann TR et al. (2012) Ages of lava flows in the Hesperia Volcanic Province, Mars. 43th LPSC, 2526
Lentz RFC, McSween HY, Ryan J, Riciputi LR (2001) Water in martian magmas: clues from light lithophile elements in shergottite and nakhlite pyroxenes. Geochim Cosmochim Acta 65:4551–4565
Magalhaes J, Gierasch P (1982) A model of Martian slope winds: Implications for eolian transport. JGR 87(B12): 9975–9984
Malin C et al. (2006) Present-Day Impact Cratering Rate and Contemporary Gully Activity on Mars. Science 314:1573–1157
Malin MC et al. (2007) Context Camera Investigation on board the Mars Reconnaissance Orbiter. JGR 112:E05S04
McEwen AS et al. (2005) The rayed crater Zunil and interpretations of small impact craters on Mars. Icarus 176:351–381
Melosh HJ (1985) Ejection of Rock Fragments from Planetary Bodies. Geol 13:144–148
Mikouchi T et al. (2003) Mineralogy and petrology of Yamato 000593: Comparison with other Martian nakhlite meteorites. Antarctic Meteorite Research 16:34–57
Morgan F, Murchie SL (2013) Fresh craters as probes of composition in dust-covered regions of Mars. 44th LPSC, 2803
Mouginis-Mark PJ et al. (1992) Martian parent craters for the SNC meteorites. JGR 97:10, 213–10, 225
Mustard JF et al. (2013) Visible-infrared reflectance of the Tissint meteorite: impact melt, maskelynite, and implications for Mars remote sensing. 44th LPSC, 2771
Nakamura N et al. (1977) Nakhla: Further Evidence for a Young Crystallization Age. Meteoritics 12:324
Nyquist LE et al. (2001) Ages and geologic histories of Martian meteorites. SSR 96:105–164
Ody A et al. (2015) Candidates source regions of martian meteorites as identified by OMEGA/MEx. Icarus 258: 366–383
Park J et al. (2009) ^{39}Ar-^{40}Ar ages of Martian nakhlites. GCA 73:2177–2189
Piatek JL et al. (2014) In search of pristine Martian impact crater ejecta deposits. 45th LPSC, 2813
Preblich BS et al. (2007) Mapping rays and secondary craters from the Martian crater Zunil. JGR 112(E5): E05006
Schon SC, Head JW (2012) Decameter-scale pedestal craters in the tropics of Mars: Evidence for the recent presence of very young regional ice deposits in Tharsis. EPSL 317–318:68–75
Tanaka KL et al. (2014) Geologic map of Mars: U.S. Geological Survey Scientific Investigations Map 3292, scale 1:20,000,000, pamphlet 43 p. doi:10.3133/sim3292
Tornabene LL (2005) Recognition of rayed craters on Mars in THEMIS thermal infrared imagery: Implications for Martian Meteorite source regions. 36th LPSC, 1970
Tornabene LL et al. (2006) Identification of large (2–10 km) rayed craters on Mars in THEMIS thermal infrared images: Implications for possible Martian meteorite source regions. JGR 111:E10006
Tornabene LL et al. (2013) A revised global depth-diameter scaling relationship for Mars based on pitted impact melt-bearing craters. 44th LPSC, 2592
Treiman AH (1993) The parent magma of the Nakhla (SNC) meteorite, inferred from magmatic inclusions. GCA 57:4753–4767
Treiman AH (2005) The nakhlite meteorites: augite-rich igneous rocks from Mars. ChemErde 65:203–270
Wadhwa M, Crozaz G (1995) Trace and minor elements in minerals of nakhlites and Chassigny: Clues to their petrogenesis. GCA 59:3629–3645
Warren PH (1994) Lunar and Martian meteorite delivery services. Icarus 111:338–363
Werner SC et al. (2014a) Mojave Crater, Mars, the Shergottites' Source Crater and Chronology Models. 77th MetSoc, 5062
Werner SC et al. (2014b) The source crater of martian shergottite meteorites. Science 343:1343–1346
Wittmann A et al. (2015) Petrography and composition of Martian regolith breccia meteorite Northwest Africa 7475. MAPS 50:326–352